Research Article

Injectable Porous Microchips with Oxygen Reservoirs and an Immune-Niche Enhance the Efficacy of CAR T Cell Therapy in Solid Tumors

Zuyuan Luo,[§] Zhen Liu,[§] Zhen Liang, Jijia Pan, Jun Xu, Jiebin Dong, Yun Bai,* Hongkui Deng,* and Shicheng Wei*

Cite This: https://dx.doi.org/10.1021/acsami.0c15239

Read Online

ACCESS | Metrics & More | Article Recommendations | Supporting Information

ABSTRACT: Chimeric antigen receptor (CAR) T cell therapy is a promising new class of hematological malignancy treatment. However, CAR T cells are rarely effective in solid tumor therapy mainly because of the poor trafficking of injected CAR T cells to the tumor site and their limited infiltration and survival in the immunosuppressive and hypoxic tumor microenvironment (TME). Here, we built an injectable immune-microchip (i-G/MC) system to intratumorally deliver CAR T cells and enhance their therapeutic efficacy in solid tumors. In the i-G/MC, oxygen carriers (Hemo) are released to disrupt the TME, and then, CAR T cells migrate from IL-15-laden i-G/MCs into the tumor stroma. The results indicate that Hemo and IL-15 synergistically enhanced CAR T cell survival and expansion under hypoxic conditions, promoting the potency and memory of CAR T cells. This i-G/MC not only serves as a cell carrier but also builds an immune-niche, enhancing the efficacy of CAR T cells.

KEYWORDS: CAR T cells, immunotherapy, solid tumors, local delivery, injectable scaffolds
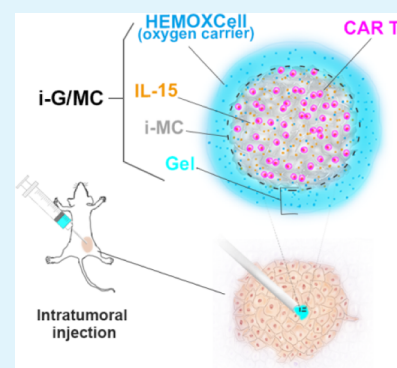
INTRODUCTION

Recently, chimeric antigen receptor (CAR) T cell therapy, which uses gene transfer technology to enable autologous T cells to express CARs,[1,2] has emerged as a powerful new class of cancer therapeutic.[3-5] Although CAR T cells consistently produce positive results in patients with hematological malignancies, thus far, they have been ineffective against solid tumors. The low efficacy of CAR T cell therapy in solid tumors is mainly attributed to the inefficient trafficking of intravenously injected CAR T cells to the tumor site, and their limited infiltration, poor survival, and proliferation in the immunosuppressive and hypoxic tumor microenvironment (TME).[6,7] Notably, these issues cannot be solved by simply increasing the number of intravenously injected CAR T cells, as this approach confers no benefits but increases the risk of side effects owing to the CAR T cells attacking vital tissues.[8,9] Therefore, novel strategies are highly needed to establish an effective CAR T cell therapy for solid tumors.

Extensive efforts have been made to overcome the limitations of CAR T cell therapy in solid tumors. To increase the infiltration rate of CAR T cells and prevent on-target/off-tumor effects, one strategy is to directly inject CAR T cells into tumor tissue by local delivery. However, the immunosuppressive and hypoxic TME of solid tumors can limit the potency and survival of CAR T cells, as oxygen and immune niches are essential to CAR T cell survival and persistence.[7,10,11] Indeed, June et al. reported the treatment of metastatic breast cancer

with intratumoral injection of CAR T cells in a phase 0 clinical trial, but the efficacy was low.[12] An alternative strategy is the use of alginate bioscaffolds to locally deliver engineered T cells to regions near solid tumors that are biocompatible with T cells and can enhance T cell survival and proliferation.[13,14] However, on-target/off-tumor effects may still occur in the vital tissues near the implantation position, and the delivered T cells may still have low rates of infiltration and survival in the immunosuppressive and hypoxic TME. Furthermore, bioscaffold implantation can also lead to surgical trauma in the body,[15] and the T cells could have low migration rate in the gel delivery systems.[16-18] To solve the abovementioned problems, an ideal strategy is to develop an injectable system with the capabilities of intratumorally delivering T cells and improving the TME to promote T cell survival and proliferation.

Herein, we developed an injectable hydrogel-encapsulated porous immune-microchip system (i-G/MC) with the capabilities of enhancing CAR T cell survival and proliferation by improving hypoxia in the TME and building an immune-
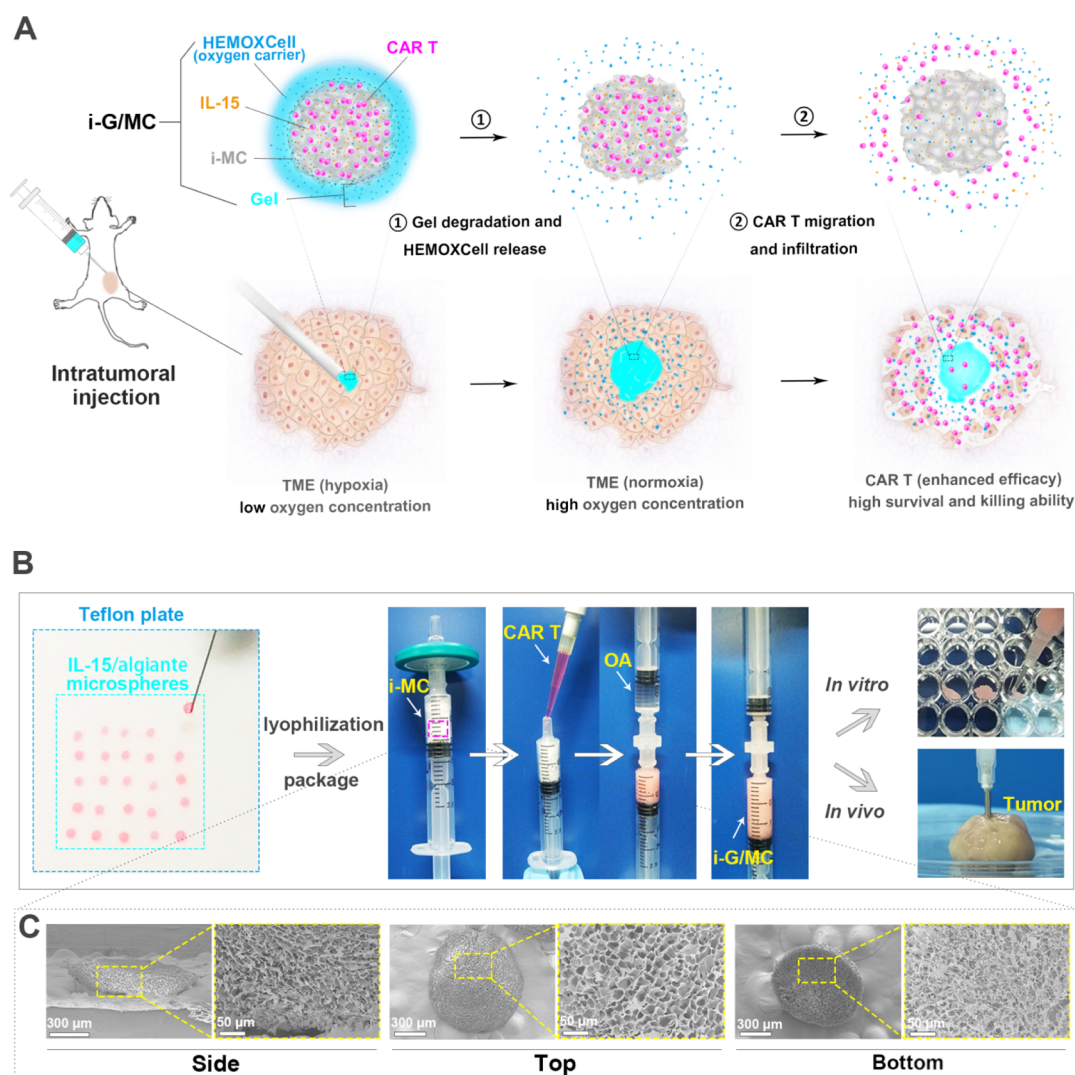
A

Figure 1. Schematic of the injectable i-G/MC system for the intratumoral delivery of CAR T cells. (A) Schematic illustration of the i-G/MC with the capability of enhancing CAR T cell survival and persistence by improving hypoxia in the TME and building an immune-niche. (B) Photographs of the preparation method used for i-G/MC production and CAR T cell encapsulation into the system. (C) SEM images of IL-15-loaded MCs.

niche to intratumorally deliver CAR T cells. The hydrogel (gel) layer that surrounds and coats the microchips (MCs) degraded quickly, delivering oxygen carriers (HEMOXCell) to the tumor stroma (Figure 1A). HEMOXCell (Hemo) is a marine extracellular hemoglobin with an outstanding oxygen storage capacity; it can bind up to 156 oxygen molecules (per Hemo molecule).[19] The sustained release of oxygen could result in high oxygen tension throughout the tumor, which is conducive to the survival of infiltrating immunocytes. Moreover, the increased oxygen tension could downregulate the expression of hypoxia-inducible factor-1α (HIF-1α), which can promote cancer progression.[20,21] In this system, CAR T cells migrated from the MCs into the tumor when the gel layer was degraded (Figure 1A). In addition, immune-MCs (i-MCs) loaded with interleukin-15 (IL-15), a potent cytokine that promotes proliferation and memory of T cells,[22,23] built an immune-niche to deliver and enhance the efficacy of CAR T cells.

■ RESULTS AND DISCUSSION

Preparation and Characterization of i-G/MC. Importantly, the carrier for intratumoral delivery of CAR T cells should have an interconnected porous structure, which is necessary for cell migration out of the carrier into the tumor. Our previous study demonstrated that small physical size of microscaffolds is beneficial for nutrient supplies and cell migration.[24] A thinner physical size of the carrier could further increase the rate of CAR T cells migrating out of the carrier. Therefore, we developed a novel and facile method to fabricate thinner carriers (MC) by freeze-drying IL-15-loaded alginate microspheres on Teflon plates (Figure 1B). Thin i-MCs (~200 μm in thickness) with highly porous interconnectivity, which was conducive to CAR T cell migration, were observed (Figure 1C). Then, HEMOXCell (Hemo; an oxygen carrier)-loaded alginate was mixed with i-MC through a female−female luer lock coupler, and the alginate self-cross-linked to form a gel layer on the i-MC via the residual Ca^{2+} in the i-MC (Figure 1B). Hemo is a marine extracellular hemoglobin with an outstanding oxygen storage capacity; it can bind up to 156 oxygen molecules (per Hemo molecule).[19]

Based on the design of the i-G/MC, the gel layer must be degraded to release Hemo at an early stage to increase the oxygen tension in the TME. As shown in Figure 2A, the porous MC (green) was encased in a uniform gel layer (red) while the
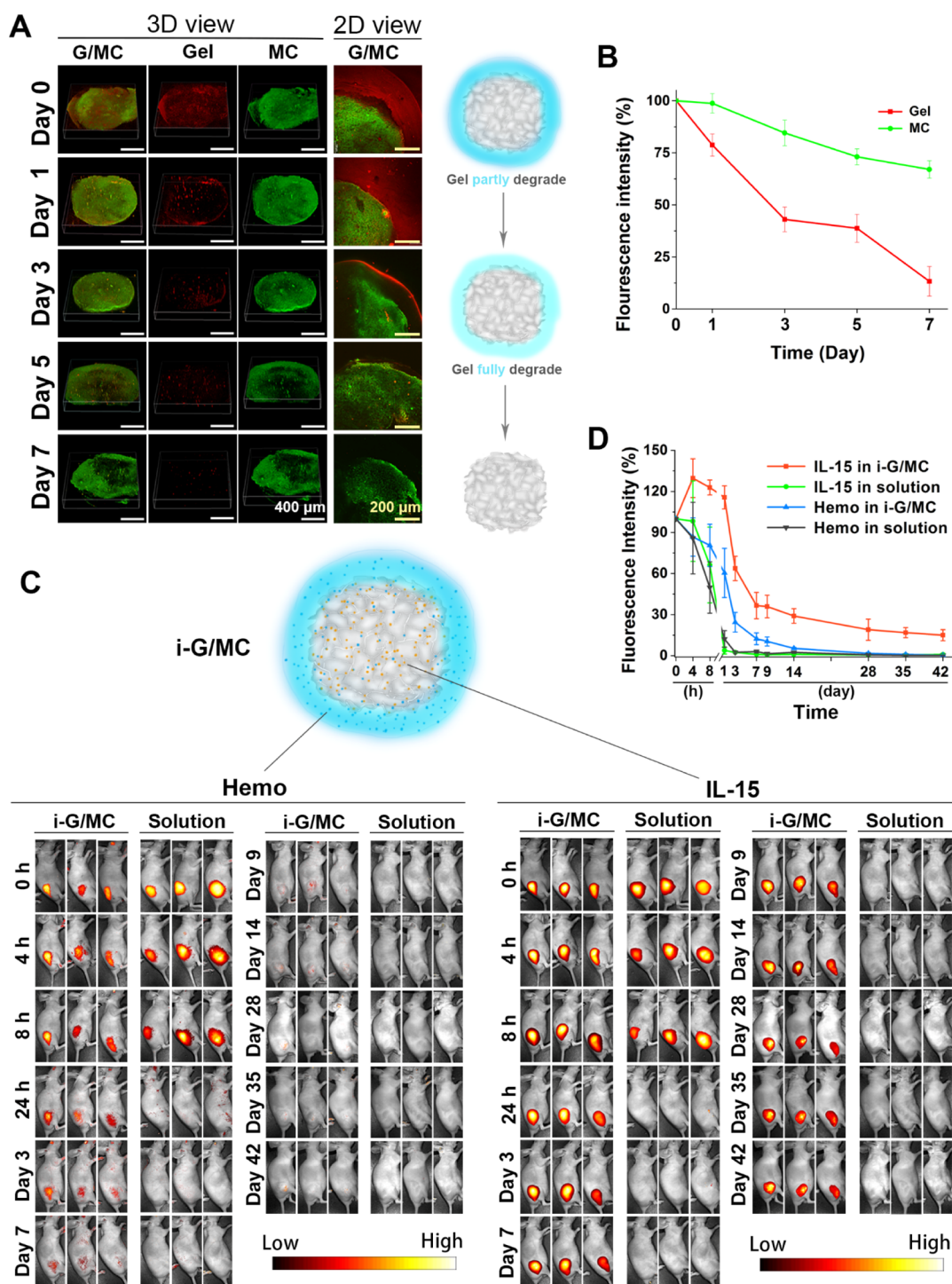
Figure 2. Characterization of the i-G/MC system and release profiles of Hemo and IL-15 from the i-G/MC *in vivo*. (A) Degradation (retained fluorescence images) of the gel layer and MCs monitored by CLSM and a schematic illustration of gel layer degradation. (B) Quantitative assessment of the retained fluorescence intensity in the gel layer and MCs. (C) Fluorescence IVIS images depicting the release profiles of molecule payloads modeling Hemo (AF594) and IL-15 (AF750) *in vivo*. (D) Quantification of the fluorescence intensity in IVIS images. All data represent the means ± SD (n = 3).

system was prepared (day 0). From both 2D and 3D views, the gel was observed around and inside the MC, indicating that the gel containing Hemo can not only deliver oxygen to the TME but also provide oxygen to CAR T cells in the i-G/MC during the initial stage. Figure 2A,B shows that the gel layer begins to degrade on day 1 and is almost completely degraded by day 7 *in vitro*. Nevertheless, the MC was stable with little degradation

for at least 7 days, during which time a strong fluorescence intensity and intact morphology were observed. When the gel layer degraded, CAR T cells migrate from the i-MC into the tumor stroma, where the oxygen tension has been enhanced. Figure S1 (Supporting Information) shows the fast gelatinization rate for the gel layer on the i-MC and the low elastic modulus for the gel layer. In fact, the rapid degradation rate of
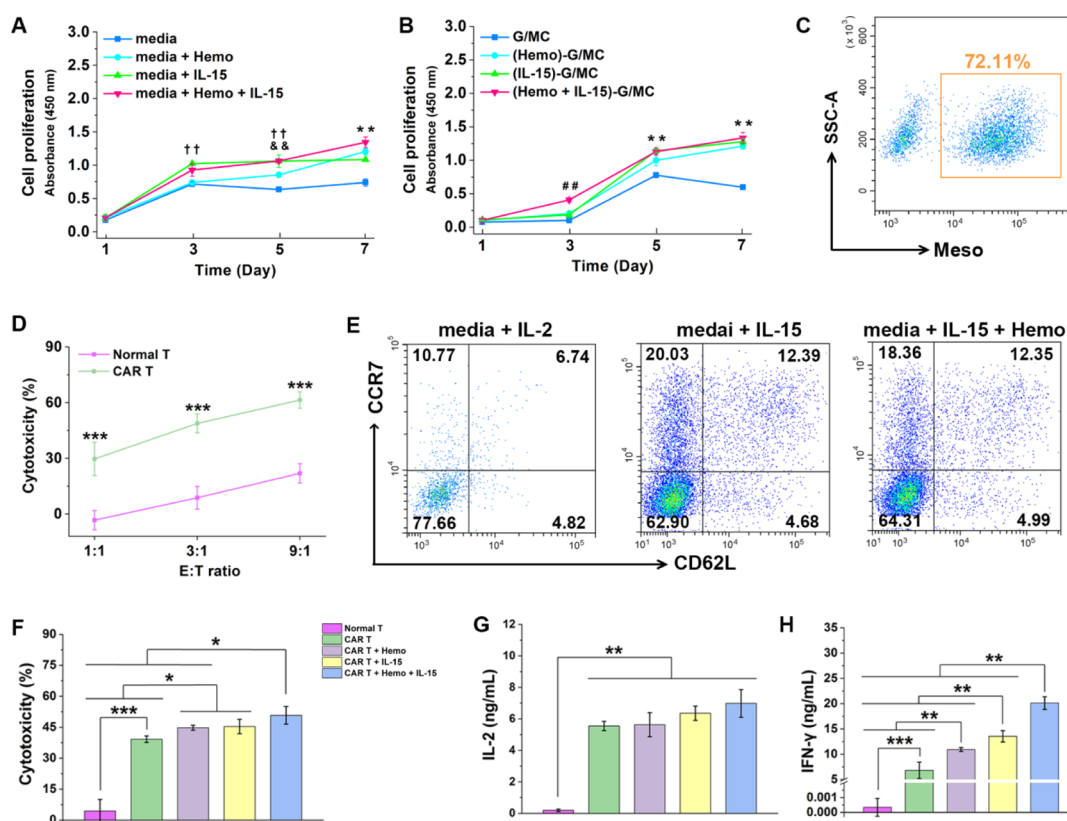
Figure 3. Preparation and evaluation of Meso-CAR T cells *in vitro*. (A) Proliferation of T cells grown in suspension culture and under hypoxic conditions (5% oxygen) with Hemo or IL-15. (B) Proliferation of T cells cultured in various MCs under hypoxic conditions (C) expression level of Meso-CAR measured by flow cytometry. (D) Cytotoxicity assay using CAR T cells co-cultured with SKOV-3 cells for 18 h. (E) Expression of CCR7 and CD62L in CAR T cells after culturing with Hemo and IL-15 under hypoxic conditions. (F) Cytotoxicity assay with CAR T cells cultured with Hemo and IL-15 under hypoxic conditions. (G) IL-2 and (H) IFN-γ release from CAR T cells detected by ELISA after a coculture with Meso$^+$ SKOV-3 cells under hypoxic conditions. *P*-values were calculated using Student's *t*-test. *$P < 0.05$, **$P < 0.01$, and ***$P < 0.001$. In A and B: $^{\dagger\dagger}P < 0.01$, medium + IL-15 and medium + IL-15 + Hemo compared to medium and medium + Hemo; $^{\&\&}P < 0.01$, medium + Hemo compared to medium alone; $^{\#\#}P < 0.01$, i-G/MC compared to other treatments; **$P < 0.01$, media or G/MC compared to others. All data represent the means ± SD ($n = 6$).

the gel layer (Figure S2) can be attributed to the small amount of cross-linkers, leading to weak cross-linking in the gel. After the lyophilized alginate, MCs were cross-linked with a CaCl$_2$ solution, most of the residual Ca^{2+} was washed away with PBS, and the degradation rate could be affected by the wash time.

The release rate of drugs was positively correlated with the degradation rate of the gel layer or the MC. To reflect the kinetics of the release of Hemo and IL-15 from the i-G/MC, we monitored the retention of these molecules *in vitro* (Figure S3) and *in vivo*. As their physical properties are similar to those of the molecules of interest, Alexa Fluor 594 IgG (AF594) and Alexa Fluor 750 IgG (AF750) were used as molecular payload models for Hemo and IL-15, respectively. For comparison, AF594 and AF750 in solution were also subcutaneously injected into tumor-free nude mice, and then, fluorescence intensity was monitored using an *in vivo* imaging system (IVIS). The fluorescence measured by the IVIS showed that approximately 15% of the signal was retained at 24 h after the administration of the two model molecules in solution (Figure 2C,D). However, the signal decay of the model molecules was significantly slower in the i-MC (42 days) than in the gel layer (7 days). The IVIS fluorescence results indicate that the i-G/MC prolonged the retention of drugs *in vivo* (compared to the retention time when the drugs were administered in a solution), whereas the retention time of drugs in the i-MC

was much longer than that in the gel layer (Figure 2C,D). Moreover, less than 30% of the model molecule signal remained in the gel layer by day 3, suggesting that most of the Hemo payload was delivered to the TME to increase the oxygen tension at an early stage, which is consistent with our proposed strategy. As shown in Figure 2C,D, the sustained and long-term release of IL-15 created an immune-niche that promoted CAR T cell proliferation.

i-G/MC Promotes the Survival and Proliferation of T Cells under Hypoxic Conditions. Before *in vivo* treatment, we tested the effects of the i-G/MC on T cell survival and proliferation under hypoxic conditions (5%) *in vitro*. Figure 3A shows the CCK-8 assay results for T cells that were directly cultured in a series of media, which exhibited that both Hemo and IL-15 were biocompatible and had no cytotoxicity to T cells. Moreover, T cells cultured in medium with IL-15 showed higher proliferative activity than those cultured in normal medium after 3 days. Many previous studies have demonstrated that IL-15 can distinctly activate T cells and stimulate T cell proliferation.[25−27] Over this time course (day 1 to day 7), T cells showed much higher activity in medium supplemented with both Hemo and IL-15 than in medium supplemented with either Hemo or IL-15 alone. These results suggest that Hemo can promote T cell survival and IL-15 can stimulate T cell proliferation in a hypoxic environment, but there was no
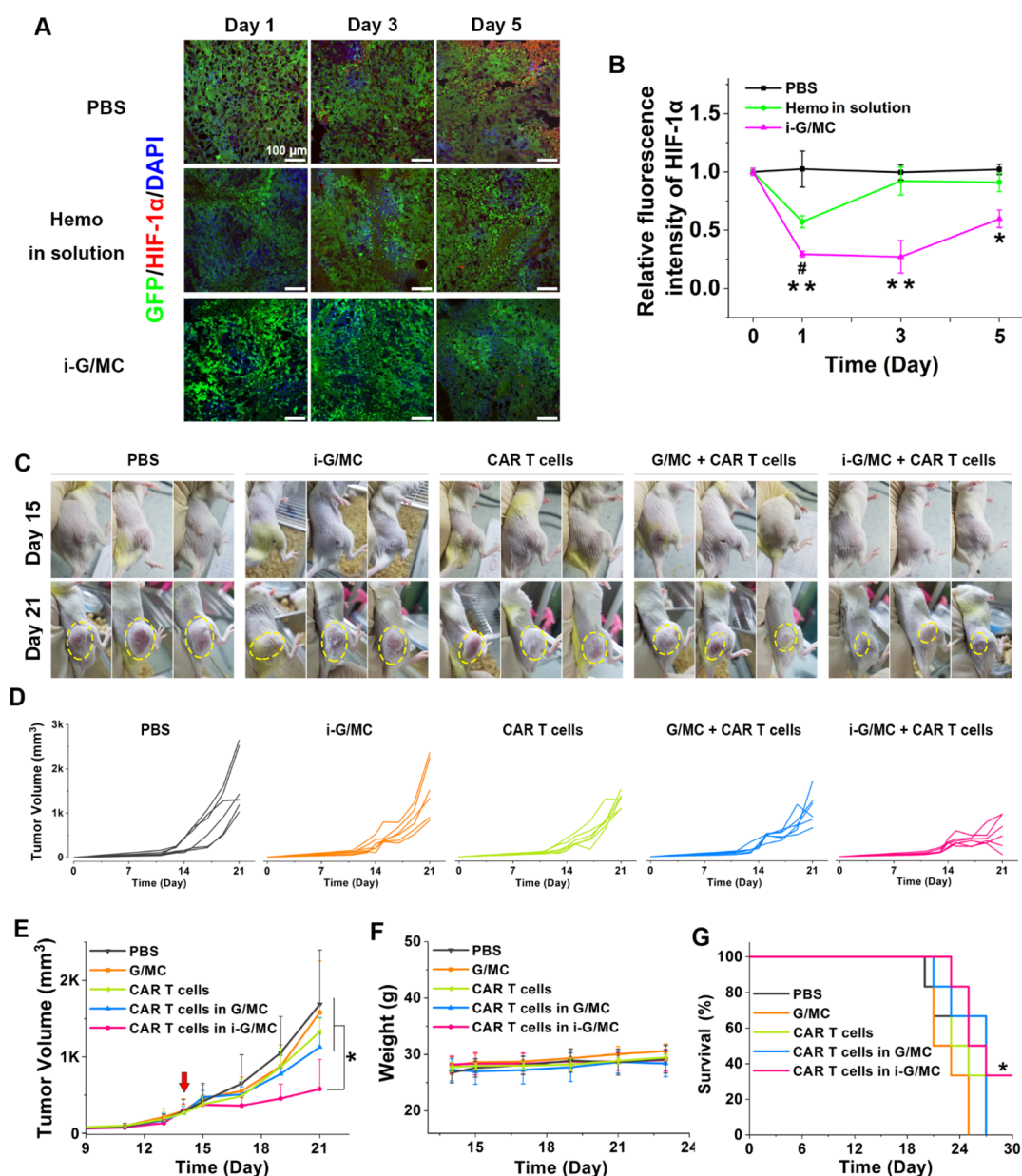
Figure 4. Antitumor efficacy of CAR T cells delivered intratumorally by the i-G/MC *in vivo*. (A) Intratumoral HIF-1α expression after injection of PBS, free Hemo (in solution), or the i-G/MC at different time points. (B) Quantification of the fluorescence intensity of HIF-1α ($n = 3$). (C) Representative images of various tumors after treatment for 1 or 7 days. (D) Individual and (E) average tumor growth ($n = 6$), (F) average body weights ($n = 6$), and (G) survival curves of various treatment groups. *P*-values were calculated using Student's *t*-test. *$P < 0.05$, **$P < 0.01$, and ***$P < 0.001$. In B: #$P < 0.05$, free Hemo compared to PBS; *$P < 0.05$, the i-G/MC compared to other treatments. All data represent the means ± SD.

effect on the proliferation of a human ovarian adenocarcinoma cell line (SKOV-3) (Figure S4, Supporting Information).

To further confirm the efficacy of the combination of Hemo and IL-15, T cells were loaded in gel-encapsulated MCs (G/MCs) with or without Hemo and IL-15 to study their activities *in vitro*. The high biocompatibility is necessary for a biomaterial, and the CCK-8 results in Figure 3B suggested that no samples had cytotoxicity. The activity of T cells in the i-G/MC (with both Hemo and IL-15) was significantly higher than that in other groups on day 3 (Figures 3B and S5). However, there were no obvious differences among G/MC loaded with Hemo and IL-15, Hemo alone, or IL-15 alone after day 5, possibly because of the degradation of the gel layer. Combined with the results shown in Figure 2A, half of the gel

layer was degraded by day 3, suggesting that there was almost no Hemo in the MC and most of the Hemo was in the medium. However, all culture media were changed every 2 days, resulting in minimal differences among the groups in terms of the amount of Hemo after day 3. Interestingly, although there was no difference in the Hemo amount between the Hemo-G/MC and G/MC groups after day 5, the cell activity in the Hemo-G/MC groups was much higher than that in the G/MC groups. As discussed in Figure 2A, Hemo in gel could not only deliver oxygen to the culture medium but also provide oxygen to T cells in the i-G/MC during the initial stage. The survival of T cells in the Hemo-G/MC groups was enhanced, whereas the lack of oxygen in the G/MC groups resulted in the death of many T cells within the first 3 days.
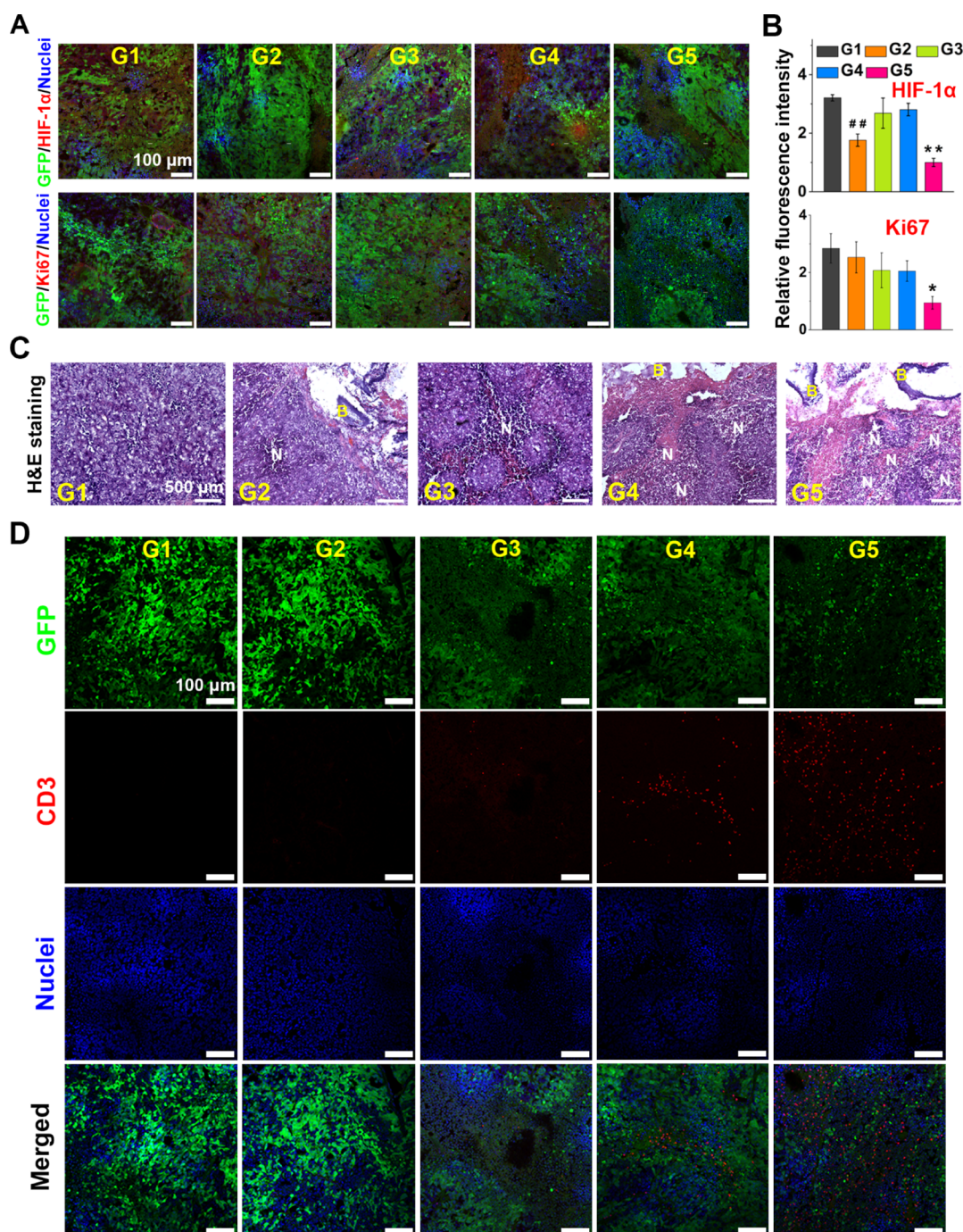
E

Figure 5. Overcoming tumor hypoxia and antitumor therapy *in vivo* for 7 days. (A) Immunofluorescence images and (B) quantification of HIF-1α and Ki67 expression in various groups. (C) H&E staining images of treated tumors (N: necrosis tumor tissue; B: biomaterials, G/MC or i-G/MC). (D) Immunofluorescence images of SKOV-3 cells and surviving CAR T cells in tumors. G1, PBS; G2, G/MC only; G3, CAR T cells only; G4, G/MC loaded with CAR T cells; and G5, i-G/MC loaded with CAR T cells. *P*-values were calculated using Student's *t*-test. *P < 0.05, **P < 0.01; ##P < 0.01, G2 compared to G1, G3, and G4. All data represent the means ± SD (n = 6).

The cell activity detected by CCK-8 is only one aspect of evaluating T cells; we next examined the ability of CAR T cells to kill tumor cells (cytotoxicity).

Combination of Hemo and IL-15 Enhances the Antitumor Efficacy of CAR T Cells *In Vitro*. In this study, human CAR T cells that targeted mesothelin (Meso) were cultured with luciferase-expressing SKOV-3 cells (Figure S6, Supporting Information). The high expression of Meso-CARs and the much higher cytotoxicity of Meso-CAR T cells (compared to normal T cells) indicated that Meso-CAR

expression by the T cells was successful (Figure 3C,D). The generation and efficient maintenance of memory CAR T cells are essential for improving immunotherapeutic efficacy,[22] and previous studies have demonstrated that IL-15 can enhance the proliferation of memory T cells.[26,27] Flow cytometry analysis results (Figure 3E) revealed higher expression of CCR7 and CD62L (two important markers of memory T cells) in CAR T cells in medium supplemented with IL-15 than CAR T cells in medium supplemented with IL-2 under hypoxic conditions. Moreover, Figure S7 shows higher expression of CCR7 and

CD62L in CAR T cells in the (IL-15)-G/MC (loaded with IL-15) than CAR T cells in G/MC under hypoxic conditions. The addition of Hemo affected on the generation and maintenance of memory CAR T cells enhanced by IL-15. When both Hemo and IL-15 were present, the survival and proliferation of memory CAR T cells was promoted, which resulted in increased cytotoxicity of the CAR T cells (Figure 3F). In the hypoxic environment, Hemo first promoted CAR T cell survival, and then, IL-15 enhanced the expansion of the surviving CAR T cells. These *in vitro* results demonstrate that the combination of Hemo and IL-15 is effective for enhancing the antitumor efficacy of CAR T cells. Furthermore, the secretion of cytokines by CAR T cells, in addition to the killing of tumor cells, also supports this conclusion (Figures 3G,H; S8, Supporting Information). Notably, the secretion of IFN-γ by T cells during tumor cell killing was affected by the CAR structure, Hemo, and IL-15. IFN-γ is a cytokine that can regulate immune-activity and has antitumor properties.[28,29] IFN-γ secretion was much higher in the CAR T cell groups (with both Hemo and IL-15) than in the other groups (Figure 3H).

i-G/MC Downregulates HIF-1α Expression and Enhances CAR T Cell Antitumor Efficacy *In Vivo*. The effect of released Hemo on the *in vivo* intratumoral hypoxia status requires further evaluation. One day after Hemo was delivered into tumors, markedly reduced hypoxia (HIF-1α) was observed (Figure 4A). In particular, the expression of HIF-1α in the i-G/MC groups was much lower than that in the free Hemo groups (Hemo in solution). Combined with the results shown in Figure 2C, Hemo in the i-G/MC had a longer release period than Hemo in solution *in vivo*. The sustained release of Hemo in tumors would provide oxygen continuously, leading to a decrease in the HIF-1α expression. Hemo is an ideal oxygen storage container with the capability of carrying 156 oxygen molecules.[19] The gel layer in the i-G/MC is a local release carrier for Hemo. As shown in Figure 4A,B, the i-G/MC could improve hypoxia in the TME (SKOV-3 tumor) for at least 5 days, which would enhance the survival of intratumorally delivered CAR T cells.

To further evaluate survival and synergistic antitumor efficacy, SKOV-3 tumor-bearing male NPG/Vst mice, the most immune-deficient mouse model,[30] were intratumorally injected with PBS, blank i-G/MC, free CAR T cells, G/MC + CAR T cells, or i-G/MC + CAR T cells. Figure 4C shows representative images of various tumors after treatment for 1 day or 7 days. The tumor sizes in the i-G/MC + CAR T cells groups were obviously smaller than those in the other groups after 7 days of treatment. Moreover, the tumor growth rates slowed after mice were treated with i-G/MC + CAR T cells for 3 days (Figure 4D,E). The tumor growth rates of the mice treated with PBS or blank i-G/MC remained high and were higher than those of the mice treated with free CAR T cells or G/MC + CAR T cells. The high growth rates of the tumors in the PBS and blank i-G/MC groups suggested that blank i-G/MC alone was not toxic to the tumor cells and could not suppress tumor progression. Although both Hemo and IL-15 were present in the i-G/MC to build an immune-niche in the tumor, there were no autologous-immunocytes in the NPG/Vst mouse model, resulting in no effector cells to kill tumor cells in these groups. We used these mice to create a mouse tumor model that evades the immune response involving autologous immunocytes and to demonstrate the i-G/MC enhancing efficacy by promoting the survival and potency of injected CAR T cells. In addition, the growth of the tumors treated with free CAR T cells or G/MC + CAR T cells was not obviously inhibited, whereas the growth rate of the tumors treated with G/MC + CAR T cells was slower than that with free CAR T cell groups (Figure 4D,E). Previous studies have reported that direct intratumoral injection of CAR T cells has no distinct efficacy because of poor cell survival and potency in tumors.[31] However, the tumor growth rate slowed after CAR T cells were encapsulated in the G/MC (compared to free CAR T cells groups), suggesting the MCs themselves (without Hemo or IL-15) have the capability to promote CAR T cell survival. Moreover, the weights of all mice were monitored and showed no differences among all groups (Figure 4F). As shown in Figure 4G, after treatment with i-G/MC + CAR T cells, the mouse survival rate was greatly improved and significantly higher than that in the other groups. The *in vivo* study demonstrated that i-G/MC + CAR T cells can inhibit tumor growth.

i-G/MC Improves the Hypoxia TEM and Promotes the Survival and Infiltration of CAR T Cells. As discussed above, Hemo can deliver sufficient oxygen into the tumor stroma to improve the hypoxic TME after intratumoral injection of the i-G/MC. Figure 5A,B shows the expression of HIF-1α and Ki67 in various groups after 7 days of treatment. Consistent with the results shown in Figure 4A, the HIF-1α expression was much lower in the groups injected with i-G/MC (G2 and G5) than that in the other groups. Interestingly, stronger fluorescence signals were observed in G5 than in G2, whereas there was no difference in the amount of Hemo between the two groups. We noted that tumor volume differed between these two groups, and the intratumoral oxygen tension decreased as the tumor volume increased.[32] Therefore, compared to G5, G2 had a larger tumor volume that resulted in a lower oxygen tension and more HIF-1α expression. Furthermore, as shown by the H&E staining results (Figure 5C), necrosis occurred in G5 and most of the tumor cells were killed (Figure 5A), which may have led to the lower HIF-1α expression in G5. The Ki67 expression levels (Figure 5A) confirmed this hypothesis. High Ki67 expression reflects a high cell proliferation rate.[33,34] There were no statistically significant differences among the groups G1, G2, G3, and G4, but obvious low expression of Ki67 was observed in G5. These results were consistent with the tumor growth and volume results in Figure 4. Clearly, the growth rate of tumor cells was suppressed after treatment with i-G/MC + CAR T cells (G5). However, the Ki67 and H&E staining results exhibited that free CAR T cells (G3) and CAR T cells in G/MC (G4) did not inhibit the proliferation of tumor cells, supporting the above findings in Figure 4.

To further investigate the therapeutic mechanism of i-G/MC + CAR T cells in tumor immunotherapy, immunofluorescence staining for human CD3 was utilized to qualitatively evaluate the survival and infiltration of injected CAR T cells in tumors. Favorably, many CD3+ T cells extensively migrated from the i-G/MC to the tumor stroma in G5 (Figures 5D; S9, Supporting Information), whereas almost no CD3+ T cell infiltration was observed in G3. These results demonstrate that the i-G/MC promoted CAR T cell survival and persistence in solid tumors. When CAR T cells are delivered into the tumor, many of them die because of the TME. Therefore, almost no CD3+ T cells were observed in the tumor injected with free CAR T cells after 7 days (Figures 5D; S10, Supporting Information). Some CD3+ T cells were found in G4, indicating

that the G/MC protected CAR T cells in the TME. During the early stage after injection, the gel-coated porous MC insulated the CAR T cells from the TME via microencapsulation. In G5, prior to the degradation of the gel layer, IL-15 stimulated CAR T cell proliferation, and then, the excited CAR T cells and oxygen migrated to the tumor when the gel layer degraded. These results demonstrate that the injectable i-G/MC enhanced the survival and efficacy of CAR T cells into solid tumors. However, the mice did not receive treatment until the tumor volume reached approximately 250 mm^3, which is a size that is difficult to be suppressed (but necessary for the intratumoral injection of the i-G/MC), leading to the inability to completely eliminate the tumors. The efficacy of this system in solid tumors may be further enhanced by combining more strategies or factors to activate endogenous immunity.

■ CONCLUSIONS

The limited infiltration and poor survival of CAR T cells in the TME lead to their low efficacy in solid tumors. Therefore, we developed a novel platform for enhancing the therapeutic efficacy of CAR T cells in solid tumors by building the i-G/MC, an innovative injectable hydrogel-encapsulated porous immune-MC system. This facile i-G/MC not only served as a cell carrier, but also built an immune-niche to enhance the survival and potency of intratumorally delivered CAR T cells with Hemo and IL-15. The combination of Hemo and IL-15 promoted cytotoxicity and memory of CAR T cells. *In vivo* studies demonstrated that the i-G/MC could deliver Hemo and IL-15 in a sustained manner and retain them for a long period, much longer than with direct injection of the two drugs. Furthermore, the histological and immunofluorescence evaluations confirmed that the i-G/MC had the ability to downregulate HIF-1α expression and enhance CAR T cell survival and persistence in tumors. This injectable system holds great potential as a local delivery platform for drugs and cells in immunotherapy or regenerative medicine.

■ MATERIALS AND METHODS

Fabrication of IL-15-Laden Porous MCs (i-MCs). Alginate microspheres were produced using the syringe and Teflon plate system (Figure 1B). Briefly, the microspheres were made with a 1.5% aqueous solution (1× PBS, pH 7.4) of sodium alginate (Sigma-Aldrich, USA) that was filter-sterilized (0.22 μm) and lyophilized. Recombinant human IL-15 (DetaiBio, China) was directly mixed into the alginate solution (300 ng/mL), and microspheres (~800 μm in diameter) were generated using a syringe with a blunt needle (30 G). Immediately after being dropped onto the Teflon plate, the microspheres were lyophilized and cross-linked with sterile a 2% CaCl$_2$ solution (Sigma-Aldrich). The cross-linked interleukin-15 (IL-15)-laden porous MCs (immune microchips, i-MCs) were immersed in a PBS buffer for 5 days, and the buffer was changed every day. Afterward, 0.8 mL of i-MCs was packed into a syringe and lyophilized again. To evaluate *in vitro* degradation of the MCs, a fluorescein isothiocyanate-labeled peptide (GGGGRGDASSP, 98% purity, ChinaPeptides) was conjugated to alginate polymers using published carbodiimide chemistry.[35] As a control, alginate solution without IL-15 was used to fabricate porous MCs. The morphology and porosity of the MC was observed by scanning electron microscopy (S-4800, Hitachi, Japan).

Preparation of Hydrogel Encapsulated i-MCs (i-G/MCs). The hydrogel around each i-MC was self-cross-linked by the residual Ca^{2+} in the i-MC. A commercial oxygen carrier (HEMOXCell; HEMARINA, France) was mixed into a 2% alginate solution to form an oxygen-enriched alginate solution (OA). Briefly, i-G/MCs were prepared by sequentially mixing 200 μL of PBS and 200 μL of

OA into syringes containing i-MC through a female−female luer lock coupler. Afterward, the mixture was cross-linked for 5 min to obtain i-G/MCs that could be extruded from the syringe. To evaluate *in vitro* degradation of the self-crosslinked hydrogel around i-MCs, a tetramethylrhodamine (TRITC)-labeled peptide (GGGGRGDASSP; 98% purity, ChinaPeptides) was conjugated to alginate polymers using published carbodiimide chemistry.[32]

***In Vitro* Evaluation of i-G/MC Degradation.** The *in vitro* degradation of fluorophore-labeled i-G/MC was monitored using confocal laser scanning microscopy (CLSM; A1R-si, Nikon, Japan) after the i-G/MCs were immersed in a PBS buffer (0.5 mL of i-G/MC in 4.5 mL of PBS). For elastic modulus measurement, i-G/MCs were subjected to an unconfined compression test (1 mm/min) in a mechanical apparatus (ElectroForce 3100, BOSE, USA) for a predetermined time.

***In Vivo* and *In Vitro* Release Study.** To study the *in vivo* release profiles of Alexa Fluor 750 IgG (a model of IL-15; ab175733, Abcam, UK) and Alexa Fluor 594 IgG (a model of Hemo; ab150116, Abcam), i-G/MCs were subcutaneously injected into BALB/c-nude mice (n = 3). For controls, solutions containing the two fluorescent molecules were subcutaneously injected. Fluorescence intensity was monitored using an *in vivo* imaging system (IVIS; Maestro 2, CRi, USA) and analyzed with Maestro2.10.0 software.

The release profiles of Alexa Fluor 750 IgG (a model of IL-15; ab175733, Abcam, UK) and Alexa Fluor 594 IgG (a model of Hemo; ab150116, Abcam) were determined using a fluorescence microplate reader (SpectraMax M5; Molecular Devices, USA). Briefly, i-G/MCs were immersed in media (pH 7.4, 37 °C) for up to 14 days. The supernatant was collected, and the released factor in solution was measured using the fluorescence microplate reader at the predetermined time points. The concentration of the two factors was calculated by comparison with the established standard curve.

Cell Lines. A human ovarian adenocarcinoma cell line (SKOV-3) and human HEK-293T cells were obtained from the National Infrastructure of Cell Line Resource (Beijing, China). All SKOV-3 cells used in this study were mesothelin (Meso) overexpressing cells (Meso$^+$). The Meso$^+$ SKOV-3 cells were transduced with a lentiviral vector containing full-length human Meso, luciferase, and a GFP cassette, which were driven by an EF-1α promoter. The SKOV-3 cells were cultivated in high-glucose DMEM (Gibco, USA) supplemented with 10% fetal bovine serum (FBS) (Gibco).

Generation of a Lentiviral Vector and Lentiviral Particle. A second-generation anti-Meso CAR recombinant lentiviral vector was designed to include the following components from 5′ to 3′: the VSVG lentiviral backbone, anti-Meso single-chain fragment variable (scFv), hinge and transmembrane regions of the CD8 molecule, cytoplasmic portions of 4-1BB, and cytoplasmic component of the CD3-ζ molecule. The Meso-specific scFv (clone number SS1) was synthesized by BGI Genomics (Beijing, China). The vector backbone (pRRLSIN.cPPT.PGK-GFP.WPRE) was a gift from Didier Trono (Addgene plasmid, no. 12252, MA, USA). The new lentiviral vector was named pRRL-EF1A-mesoCAR-GFP. To produce lentiviral particles, 8 × 10^6 HEK-293T cells in a 10 cm dish were co-transfected with 16 μg of lentivirus vector DNA, 12 μg of packaging vector DNA (pSPAX2), and 4 μg of envelope DNA (pMD2.G). The medium was changed to fresh high-glucose DMEM (Gibco) supplemented with 10% FBS (HyClone, Logan, UT) after 12 h, and the cells were incubated for another 24−48 h. The supernatant containing the lentiviral particles was collected and filtered through 0.22 μm polyvinylidene fluoride filters (Millipore, USA) to remove cellular debris. The lentiviral supernatant was stored at −80 °C.

Preparation of CAR T Cells. All peripheral blood mononuclear cells (PBMCs) used in our study were obtained from healthy donors who provided informed consent (Blood Center of Beijing Red Cross Society). Human PBMCs were isolated by density gradient centrifugation with a human lymphocyte separation medium (DAKAWE, China) and activated using anti-CD3/anti-CD28 beads at a concentration of three beads/cell in X-VIVO 15 medium (Lonza, USA) with 10% FBS containing 100 U/ml IL-2 at 37 °C and 5% CO$_2$ for 1−2 days. After activation, 8 μg/mL polybrene (Millipore, USA)

was added to each well, and the T cells were transduced twice over the next 24 h with the Meso-CAR lentivirus by spinoculation for 1 h. The transfected T cells were cultured in fresh culture medium at 37 °C and 5% CO_2.

Flow Cytometry. Flow cytometry was performed using a CytoFLEX platform (Beckman Coulter, USA) and CytExpert software. All cells in culture were washed with PBS before staining with antibodies. After a 30−45 min incubation at 4 °C in the dark, cells were washed twice with PBS (Gibco, USA) and analyzed with the CytoFLEX instrument. The Meso-CAR GFP expression was monitored by flow cytometry analysis of the GFP expression. Stained untransduced T cells and isotype antibodies were used as controls. CD62L and CCR7 expressions by T cells after culture under different conditions were monitored by flow cytometry using CD62L-PE and CCR7-PC5.5-A antibodies (BD, USA).

Cytotoxicity Assay. The ability of Meso-CAR T cells to lyse target tumor cells was measured using a bioluminescence assay as previously described.[36] In these assays, after culturing under different conditions for 1 week, 1×10^5, 3×10^5, and 9×10^5 cells/mL Meso-CAR T cells or T cells were co-incubated with luciferase-expressing target tumor cells (1×10^5 cells/mL) at various effector-to-target (E:T) ratios in 10% FBS-X-VIVO 15 medium in 96-well U-bottom plates for 18 h. Lysis percentages were determined using the following equation: % specific lysis = $100 \times$ (spontaneous death RLU − test RLU)/(spontaneous death RLU). RLU, relative light units.

Cytokine Production. Duplicate wells containing 5×10^4 genetically engineered Meso-CAR T cells were co-incubated with 10^5 SKOV-3-meso tumor cells in 100 μL of 10% FBS-X-VIVO 15 medium for 18 h. The cell-free supernatants were collected and assayed for IFN-γ and IL-2 cytokine content using a human IFN-γ precoated enzyme-linked immunosorbent assay (ELISA) kit and a human IL-2 precoated ELISA kit (DAKAWE, China).

Proliferation of T Cells in MCs under Hypoxic Conditions. A total of 200 μL of T cell suspension (2×10^7 cells/mL) was inoculated into MCs that were loaded in a syringe (Figure 1B). The cells were allowed to infuse into these MCs for 5 min, and then, 200 μL of alginate hydrogels (with or without O_2 carriers) was mixed into these syringes as described above. Afterward, these T cell-loaded hydrogel-encapsulated MCs were injected into a 24-well plate (25 μL/well) and cultured with base X-VIVO medium (1 mL/well). These samples were cultured under hypoxic conditions (THERMO Heracell VIOS 160i; 5% O_2 and 5% CO_2 at 37 °C). The proliferation of the T cells was tested using CCK-8 (Dojindo, Japan). Briefly, after culturing for 1, 3, 5, or 7 days, CCK-8 was added into each well for 4 h, and the absorbance value (450 nm) was determined using a microplate reader (SpectraMax i3, Molecular Devices).

Tumor Model. All animal experiments described in the present study were reviewed and approved by the Animal Care and Use Committee of Peking University. Male combined immune deficiency NPG/Vst mice (4−6 weeks of age) were obtained from VITAL-START (Beijing, China). NPG/Vst mice are members of the NOD-Prkdc[scid] Il2rg[null] family; this strain has been internationally recognized as the highest immune deficient mouse model and is therefore the most suitable tool for cell transplantation. Suspensions of 5×10^6 SKOV-3 (GFP^{+}) cells in 100 μL of PBS were subcutaneously injected onto the right back of each mouse to establish the tumor model.

***In Vivo* Therapy Study.** Therapy began when tumor volumes reached approximately 250 mm³, and the mice were randomly divided into five groups (*n* = 6). Different therapy formulations (50 μL) were injected intratumorally, and the different treatment groups were as follows: (G1) PBS, (G2) G/MC only, (G3) CAR T cells only, (G4) G/MC loaded with CAR T cells, and (G5) i-G/MC loaded with CAR T cells. The total number of intratumorally injected cells was 1×10^7 cells/tumor (Meso-CAR^{+} T cells accounted for approximately 72.11% of the cells) in all the CAR T cell therapy groups. Body weight and tumor size (monitored using a digital caliper) were measured every two days. Tumor volume was calculated using the following formula: volume = (length × width²)/2. The mice were euthanized when they became moribund or when the tumor volume exceeded 1500 mm³.

Histological Assay. Mice were sacrificed at a predetermined time, and tumors were collected for immunofluorescence and hematoxylin and eosin (H&E) staining (frozen sections). To evaluate the influence of Hemo on intratumoral hypoxia, sections were incubated with an anti-HIF-1α antibody (1:200, ab1, Abcam) and a TRITC-labeled secondary antibody (1:200, ab6786, Abcam). The proliferation of tumor cells was detected by an incubation with an anti-Ki67 antibody (1:200, ab92742, Abcam) and TRITC-labeled secondary antibody (ab6786). To evaluate the survival of intratumoral CAR T cells, sections were stained with an anti-human CD3 antibody (1:200, ab699, Abcam) and a TRITC-labeled secondary antibody (ab6786). In addition, cell nuclei were stained with DAPI (5 μg/mL, Sigma-Aldrich). The stained samples were imaged using CLSM (A1R-si, Nikon), and the fluorescence intensity and cell number were quantified using ImageJ software.

Statistical Analyses. Statistical analyses were performed using SPSS (version 24) software. Student's *t*-test was used to determine statistical significance when comparing two groups. For survival analysis, statistical differences were determined with the log-rank test.

■ ASSOCIATED CONTENT

Ⓢ Supporting Information

The Supporting Information is available free of charge at https://pubs.acs.org/doi/10.1021/acsami.0c15239.

> Elastic modulus of i-G/MC and gel layer changing with time; IL-15 and Hemo release profiles of i-G/MC in vitro; proliferation of SKOV-3 cells cultured in hypoxia condition (5% oxygen) with Hemo or IL-15, CFSE proliferation profiles of CAR T cells cultured in various conditions for 3 days, expression levels of Meso-SKOV-3 cells measured by flow cytometry, expression of CCR7 and CD62L in CAR T cells after co-culturing in G/MC with or without Hemo and IL-15 under hypoxic conditions, media with Hemo or/and IL-15 as blank control groups for cytotoxicity assay, IL-2 release, and IFN-γ release in CAR T cells, immunofluorescence images of SKOV-3 cells (GFP) and surviving CAR T cells (CD3) in the tumor, quantification of CD3^{+} T cell numbers, G1, PBS; G2, G/MC only; G3, CAR T cells only; G4, G/MC loaded with CAR T cells; G5, i-G/MC loaded with CAR T cells, and *P*-values calculated using Student's *t*-test, *P < 0.05 and **P < 0.01 (PDF)

■ AUTHOR INFORMATION

Corresponding Authors

Yun Bai − *Central Laboratory, and Department of Oral and Maxillofacial Surgery, School and Hospital of Stomatology, Peking University; Peking University Department of Cell Biology and Stem Cell Research Center, School of Basic Medical Sciences, Center for Molecular and Translational Medicine, Peking University Health Science Center, Beijing 100081, P.R. China*; Email: baiyun@bjmu.edu.cn

Hongkui Deng − *Central Laboratory, and Department of Oral and Maxillofacial Surgery, School and Hospital of Stomatology, Peking University; Peking University Department of Cell Biology and Stem Cell Research Center, School of Basic Medical Sciences, Center for Molecular and Translational Medicine, Peking University Health Science Center, Beijing 100081, P.R. China*;
Email: hongkui_deng@pku.edu.cn

Shicheng Wei − *Central Laboratory, and Department of Oral and Maxillofacial Surgery, School and Hospital of Stomatology, Peking University; Peking University Department of Cell Biology and Stem Cell Research Center,*

School of Basic Medical Sciences, Center for Molecular and Translational Medicine, Peking University Health Science Center, Beijing 100081, P.R. China; Laboratory for Biomaterials and Regenerative Medicine, Academy for Advanced Interdisciplinary Studies, Peking University, Beijing 100871, P.R. China; ● orcid.org/0000-0001-6024-9615; Email: sc-wei@pku.edu.cn

Authors

Zuyuan Luo − Central Laboratory, and Department of Oral and Maxillofacial Surgery, School and Hospital of Stomatology, Peking University; Peking University Department of Cell Biology and Stem Cell Research Center, School of Basic Medical Sciences, Center for Molecular and Translational Medicine, Peking University Health Science Center, Beijing 100081, P.R. China; Laboratory for Biomaterials and Regenerative Medicine, Academy for Advanced Interdisciplinary Studies, Peking University, Beijing 100871, P.R. China

Zhen Liu − Central Laboratory, and Department of Oral and Maxillofacial Surgery, School and Hospital of Stomatology, Peking University; Peking University Department of Cell Biology and Stem Cell Research Center, School of Basic Medical Sciences, Center for Molecular and Translational Medicine, Peking University Health Science Center, Beijing 100081, P.R. China

Zhen Liang − Central Laboratory, and Department of Oral and Maxillofacial Surgery, School and Hospital of Stomatology, Peking University; Peking University Department of Cell Biology and Stem Cell Research Center, School of Basic Medical Sciences, Center for Molecular and Translational Medicine, Peking University Health Science Center, Beijing 100081, P.R. China

Jijia Pan − Laboratory for Biomaterials and Regenerative Medicine, Academy for Advanced Interdisciplinary Studies, Peking University, Beijing 100871, P.R. China

Jun Xu − Central Laboratory, and Department of Oral and Maxillofacial Surgery, School and Hospital of Stomatology, Peking University; Peking University Department of Cell Biology and Stem Cell Research Center, School of Basic Medical Sciences, Center for Molecular and Translational Medicine, Peking University Health Science Center, Beijing 100081, P.R. China

Jiebin Dong − Central Laboratory, and Department of Oral and Maxillofacial Surgery, School and Hospital of Stomatology, Peking University; Peking University Department of Cell Biology and Stem Cell Research Center, School of Basic Medical Sciences, Center for Molecular and Translational Medicine, Peking University Health Science Center, Beijing 100081, P.R. China

Complete contact information is available at:
https://pubs.acs.org/10.1021/acsami.0c15239

Author Contributions

§Zuyuan Luo and Zhen Liu contributed equally.

Notes

The authors declare no competing financial interest.

■ REFERENCES

(1) Barrett, D. M.; Singh, N.; Porter, D. L.; Grupp, S. A.; June, C. H. Chimeric Antigen Receptor Therapy for Cancer. Annu. Rev. Med. 2014, 65, 333−347.

(2) Lim, W. A.; June, C. H. The Principles of Engineering Immune Cells to Treat Cancer. Cell 2017, 168, 724−740.

(3) June, C. H.; O'Connor, R. S.; Kawalekar, O. U.; Ghassemi, S.; Milone, M. C. CAR T Cell Immunotherapy for Human Cancer. Science 2018, 359, 1361−1365.

(4) Kochenderfer, J. N.; Wilson, W. H.; Janik, J. E.; Dudley, M. E.; Stetler-Stevenson, M.; Feldman, S. A.; Maric, I.; Raffeld, M.; Nathan, D.-A. N.; Lanier, B. J.; Morgan, R. A.; Rosenberg, S. A. Eradication of B-lineage Cells and Regression of Lymphoma in a Patient Treated with Autologous T cells Genetically Engineered to Recognize CD19. Blood 2010, 116, 4099−4102.

(5) Grupp, S. A.; Kalos, M.; Barrett, D.; Aplenc, R.; Porter, D. L.; Rheingold, S. R.; Teachey, D. T.; Chew, A.; Hauck, B.; Wright, J. F.; Milone, M. C.; Levine, B. L.; June, C. H. Chimeric Antigen Receptor-modified T Cells for Acute Lymphoid Leukemia. N. Engl. J. Med. 2013, 368, 1509−1518.

(6) Binnewies, M.; Roberts, E. W.; Kersten, K.; Chan, V.; Fearon, D. F.; Merad, M.; Coussens, L. M.; Gabrilovich, D. I.; Ostrand-Rosenberg, S.; Hedrick, C. C.; Vonderheide, R. H.; Pittet, M. J.; Jain, R. K.; Zou, W.; Howcroft, T. K.; Woodhouse, E. C.; Weinberg, R. A.; Krummel, M. F. Understanding the Tumor Immune Microenvironment (TIME) for Effective Therapy. Nat. Med. 2018, 24, 541−550.

(7) Zou, W. Immunosuppressive Networks in the Tumour Environment and Their Therapeutic Relevance. Nat. Rev. Cancer 2005, 5, 263−274.

(8) Bonifant, C. L.; Jackson, H. J.; Brentjens, R. J.; Curran, K. J. Toxicity and Management in CAR T-cell Therapy. Mol. Ther.−Oncolytics 2016, 3, 16011−16017.

(9) Namuduri, M.; Brentjens, R. J. Medical Management of Side Effects Related to CAR T Cell Therapy in Hematologic Malignancies. Expet Rev. Hematol.. 2016, 9, 511−513.

(10) Nagarsheth, N.; Wicha, M. S.; Zou, W. Chemokines in the Cancer Microenvironment and Their Relevance in Cancer Immunotherapy. Nat. Rev. Immunol. 2017, 17, 559−572.

(11) Rankin, E. B.; Giaccia, A. J. Hypoxic Control of Metastasis. Science 2016, 352, 175−180.

(12) Tchou, J.; Zhao, Y.; Levine, B. L.; Zhang, P. J.; Davis, M. M.; Melenhorst, J. J.; Kulikovskaya, I.; Brennan, A. L.; Liu, X.; Lacey, S. F.; Posey, A. D., Jr.; Williams, A. D.; So, A.; Conejo-Garcia, J. R.; Plesa, G.; Young, R. M.; McGettigan, S.; Campbell, J.; Pierce, R. H.; Matro, J. M.; DeMichele, A. M.; Clark, A. S.; Cooper, L. J.; Schuchter, L. M.; Vonderheide, R. H.; June, C. H. Safety and Efficacy of Intratumoral Injections of Chimeric Antigen Receptor (CAR) T Cells in Metastatic Breast Cancer. Cancer Immunol. Res. 2017, 5, 1152−1161.

(13) Stephan, S. B.; Taber, A. M.; Jileaeva, I.; Pegues, E. P.; Sentman, C. L.; Stephan, M. T. Biopolymer Implants Enhance the Efficacy of Adoptive T-cell Therapy. Nat. Biotechnol. 2015, 33, 97−101.

(14) Smith, T. T.; Moffett, H. F.; Stephan, S. B.; Opel, C. F.; Dumigan, A. G.; Jiang, X.; Pillarisetty, V. G.; Pillai, S. P. S.; Wittrup, K. D.; Stephan, M. T. Biopolymers Codelivering Engineered T Cells and STING Agonists Can Eliminate Heterogeneous Tumors. J. Clin. Invest. 2017, 127, 2176−2191.

(15) Montgomery, M.; Ahadian, S.; Davenport Huyer, L.; Lo Rito, M.; Civitarese, R. A.; Vanderlaan, R. D.; Wu, J.; Reis, L. A.; Momen, A.; Akbari, S.; Pahnke, A.; Li, R.-K.; Caldarone, C. A.; Radisic, M. Flexible Shape-memory Scaffold for Minimally Invasive Delivery of Functional Tissues. Nat. Mater. 2017, 16, 1038−1046.

(16) Hori, Y.; Winans, A. M.; Huang, C. C.; Horrigan, E. M.; Irvine, D. J. Injectable dendritic cell-carrying alginate gels for immunization and immunotherapy. Biomaterials 2008, 29, 3671−3682.

(17) Yang, P.; Song, H.; Qin, Y.; Huang, P.; Zhang, C.; Kong, D.; Wang, W. Engineering dendritic cells-based vaccines and PD-1 blockade in self-assembled peptide nanofibrous hydrogel to amplify antitumor T-cell immunity. Nano Lett. 2018, 18, 4377−4385.

(18) Monette, A.; Ceccaldi, C.; Assaad, E.; Lerouge, S.; Lapointe, R. Chitosan thermogels for local expansion and delivery of tumor-specific T lymphocytes towards enhanced cancer immunotherapies. *Biomaterials* **2016**, *75*, 29237−29249.

(19) Rodriguez-Brotons, A.; Bietiger, W.; Peronet, C.; Langlois, A.; Magisson, J.; Mura, C.; Sookhareea, C.; Polard, V.; Jeandidier, N.; Zal, F.; Pinget, M.; Sigrist, S.; Maillard, E. Comparison of Perfluorodecalin and HEMOXCell as Oxygen Carriers for Islet Oxygenation in an In Vitro Model of Encapsulation. *Tissue Eng., Part A* **2016**, *22*, 1327−1336.

(20) Schito, L.; Semenza, G. L. Hypoxia-Inducible Factors: Master Regulators of Cancer Progression. *Trends Cancer* **2016**, *2*, 758−770.

(21) Harris, A. L. Hypoxia−a Key Regulatory Factor in Tumour Growth. *Nat. Rev. Cancer* **2002**, *2*, 38−47.

(22) Golubovskaya, V.; Wu, L. Different Subsets of T Cells, Memory, Effector Functions, and CAR-T Immunotherapy. *Cancers* **2016**, *8*, 2072−6694.

(23) Berard, M.; Tough, D. F. Qualitative Differences Between Naive and Memory T Cells. *Immunology* **2002**, *106*, 127−138.

(24) Luo, Z.; Pan, J.; Sun, Y.; Zhang, S.; Yang, Y.; Liu, H.; Li, Y.; Xu, X.; Sui, Y.; Wei, S. Injectable 3D Porous Micro-scaffolds with a Bio-engine for Cell Transplantation and Tissue Regeneration. *Adv. Funct. Mater.* **2018**, *28*, 1804335−1804347.

(25) Cao, P.; Chang, D. K.; Rakestraw, A.; Shaw, A.; Pucci, F.; Fachin, F.; McInnis, C.; Carey, S.; Boesch, A.; Chirgwin, D. *Am. Assoc. Cancer Res.* **2018**, *78*, 3577.

(26) Lodolce, J. P.; Boone, D. L.; Chai, S.; Swain, R. E.; Dassopoulos, T.; Trettin, S.; Ma, A. IL-15 Receptor Maintains Lymphoid Homeostasis by Supporting Lymphocyte Homing and Proliferation. *Immunity* **1998**, *9*, 669−676.

(27) Tan, J. T.; Ernst, B.; Kieper, W. C.; LeRoy, E.; Sprent, J.; Surh, C. D. Interleukin (IL)-15 and IL-7 Jointly Regulate Homeostatic Proliferation of Memory Phenotype CD8+ Cells but are not Required for Memory Phenotype CD4+ Cells. *J. Exp. Med.* **2002**, *195*, 1523−1532.

(28) Okamura, H.; Tsutsui, H.; Komatsu, T.; Yutsudo, M.; Hakura, A.; Tanimoto, T.; Torigoe, K.; Okura, T.; Nukada, Y.; Hattori, K.; Akita, K.; Namba, M.; Tanabe, F.; Konishi, K.; Fukuda, S.; Kurimoto, M. Cloning of a New Cytokine that Induces IFN-gamma Production by T Cells. *Nature* **1995**, *378*, 88−91.

(29) Mumberg, D.; Monach, P. A.; Wanderling, S.; Philip, M.; Toledano, A. Y.; Schreiber, R. D.; Schreiber, H. CD4(+) T Cells Eliminate MHC Class II-negative Cancer Cells in Vivo by Indirect Effects of IFN-gamma. *Proc. Natl. Acad. Sci. U.S.A.* **1999**, *96*, 8633−8638.

(30) Bai, Y.; Kan, S.; Zhou, S.; Wang, Y.; Xu, J.; Cooke, J. P.; Wen, J.; Deng, H. Enhancement of the in Vivo Persistence and Antitumor Efficacy of CD19 Chimeric Antigen Receptor T cells Through the Delivery of Modified TERT mRNA. *Cell Discovery* **2015**, *1*, 15040−15054.

(31) Zhang, L.; Conejo-Garcia, J. R.; Katsaros, D.; Gimotty, P. A.; Massobrio, M.; Regnani, G.; Makrigiannakis, A.; Gray, H.; Schlienger, K.; Liebman, M. N.; Rubin, S. C.; Coukos, G. Intratumoral T Cells, Recurrence, and Survival in Epithelial Ovarian Cancer. *N. Engl. J. Med.* **2003**, *348*, 203−213.

(32) Tredan, O.; Galmarini, C. M.; Patel, K.; Tannock, I. F. Drug Resistance and the Solid Tumor Microenvironment. *J. Natl. Cancer Inst.* **2007**, *99*, 1441−1454.

(33) Katzenberger, T.; Petzoldt, C.; Höller, S.; Mäder, U.; Kalla, J.; Adam, P.; Ott, M. M.; Müller-Hermelink, H. K.; Rosenwald, A.; Ott, G. The Ki67 Proliferation Index is a Quantitative Indicator of Clinical Risk in Mantle Cell Lymphoma. *Blood* **2006**, *107*, 3407.

(34) Sawhney, N.; Hall, P. A. Ki67−structure, Function, and New Antibodies. *J. Phytopathol.* **1992**, *168*, 161−162.

(35) Rowley, J. A.; Madlambayan, G.; Mooney, D. J. Alginate Hydrogels as Synthetic Extracellular Matrix Materials. *Biomaterials* **1999**, *20*, 45−53.

(36) Fu, X.; Tao, L.; Rivera, A.; Williamson, S.; Song, X.-T.; Ahmed, N.; Zhang, X. A Simple and Sensitive Method for Measuring Tumor-specific T cell Cytotoxicity. *PLoS One* **2010**, *5*, No. e11867.